isvr Institute of Sound and Vibration Research

Parametric Adaptation Algorithm for Feedback Cancellation

J.L. Hayes and B. Rafaely

ISVR Technical Memorandum 871

October 2001

University of Southampton

SCIENTIFIC PUBLICATIONS BY THE ISVR

Technical Reports are published to promote timely dissemination of research results by ISVR personnel. This medium permits more detailed presentation than is usually acceptable for scientific journals. Responsibility for both the content and any opinions expressed rests entirely with the author(s).

Technical Memoranda are produced to enable the early or preliminary release of information by ISVR personnel where such release is deemed to the appropriate. Information contained in these memoranda may be incomplete, or form part of a continuing programme; this should be borne in mind when using or quoting from these documents.

Contract Reports are produced to record the results of scientific work carried out for sponsors, under contract. The ISVR treats these reports as confidential to sponsors and does not make them available for general circulation. Individual sponsors may, however, authorize subsequent release of the material.

UNIVERSITY OF SOUTHAMPTON
INSTITUTE OF SOUND AND VIBRATION RESEARCH
SIGNAL PROCESSING & CONTROL GROUP

Parametric Adaptation Algorithm for Feedback Cancellation

by

Joanna L Hayes and Boaz Rafaely

ISVR Technical MemorandumNo. 871

October 2001

Authorised for issue by
Prof S J Elliott
Group Chairman

Abstract

A novel method of parametric adaptation for feedback cancellation has been introduced. Knowledge of the hearing aid system gained from previous modelling work was used to identify those parameters which are likely to vary after fitting the hearing aid to the user. These parameters are adapted to produce finite impulse response (FIR) filters modelling the actual feedback path response. Simulations have shown that the algorithm converges to a good estimate of the actual feedback path in far fewer iterations than the normalised least mean squares algorithm. The next stage of the work will extend the algorithm to adapt more than one parameter simultaneously and improve its computational efficiency with a view to developing a practical real-time system.

Introduction

Feedback is a major problem for hearing aid users. This is the oscillation or "whistling" that occurs when an amplified signal is fedback from the output of the hearing aid receiver (loudspeaker) to the microphone, driving the device into instability. This effect can be prevented by reducing the gain of the hearing aid, but this prevents the user obtaining full benefit from the device. This is especially so for patients with severe or profound hearing losses, who require higher gains.

A better approach is to cancel the feedback signal. This can be done by using adaptive filtering techniques to model the response of the feedback signal and then subtract this modelled response from the input to the hearing aid processing, so that the forward response, i.e. the amplified desired signal, remains (figure 1). The feedback path varies with time, so the feedback cancellation system must be adaptive.

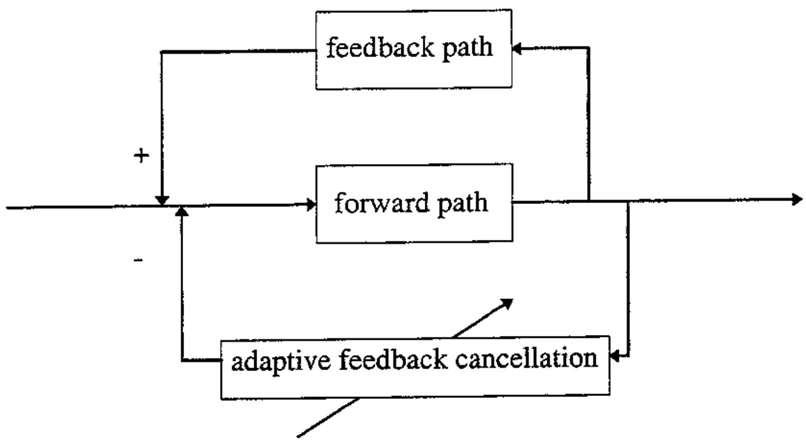

Figure 1: Schematic diagram of hearing aid with adaptive feedback cancellation.

Currently, most methods of feedback cancellation are based on the least mean squares (LMS) algorithm [Widrow and Sterns, 1985]. This method assumes no prior knowledge of the system and may take many iterations to converge. This limits the ability of the adaptive filter to track sudden changes in the feedback path.

The method of feedback cancellation proposed in this memorandum uses prior knowledge of the hearing aid system to obtain an initial response closer to that of the actual feedback path. This parametric algorithm has been shown to adapt quickly to changes in the feedback path with fast convergence which compares favourably to the LMS algorithm. This method is currently in the early stages of development. This memorandum is a summary of the work completed to date.

The hearing aid model

A comprehensive model of an *in situ* in-the-ear (ITE) hearing aid has been developed. This combines the manufacturer's electrical transducer analogues implemented with the PSpice circuit simulator [LoPresti and Carlson, 1999] with acoustic theory implemented in MATLAB. This allows variation of the transducers and the dimensions of the tubes within the system to simulate a wide range of devices and subjects. Two-port network theory was used to derive an expression for the feedback path response [Egolf *et al.*, 1989]. The model was verified experimentally for simple transducer-tube systems and with actual feedback path measurements.

Adaptive algorithms

Adaptive algorithms are used often to minimise some cost function relative to some varying parameter. A common cost function is the mean square error.

The most widely used method of adapting a parameter to minimise the cost function is the method of steepest descent. This has the form:
new parameter = old parameter - μ x (local gradient)

μ is the convergence coefficient, which governs the rate of convergence.

The local gradient is given by $\left.\dfrac{\partial(\text{cost function})}{\partial(\text{parameter})}\right|_{\text{current parameter values}}$

For this algorithm to converge reliably, the error surface obtained by plotting the cost function against the varying parameters must have a global (i.e. unique) minimum and the convergence coefficient α must be large but not too large.

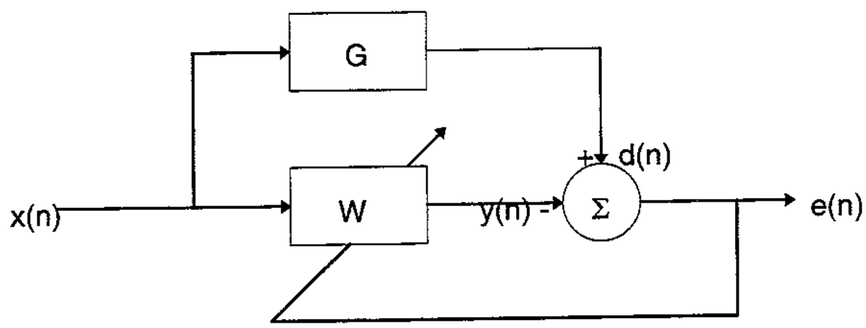

Figure 2: Block diagram of an adaptive system

Consider the system in figure 2. The input signal $\mathbf{x}(n)$ is filtered by the feedback path, G, to give the desired signal, $d(n)$. The input signal is filtered also by the adaptive filter, W, with coefficients w_i, to give the estimate of the desired signal, $y(n)$. The error signal, $e(n)$, is given by

$$e(n) = d(n) - y(n) = d(n) - \mathbf{w}^T(n)\mathbf{x}(n) \tag{1}$$

We wish to minimise the error signal, $e(n)$, so that the adaptive filter converges to give the same response as the feedback path. The mean square error, $E[e^2(n)]$ is a suitable cost function.

The convergence coefficient α should be chosen with care. If α is too small, the filter will take a long time to converge to the correct solution and will be poor at tracking changes. If α is large, the solution will be reached quickly, but if α is too large, the filter will overshoot the solution and will take a long time to converge.

Least mean squares algorithm

The least mean squares (LMS) algorithm updates the adaptive filter coefficients according to equation (2).

$$\mathbf{w}(n+1) = \mathbf{w}(n) + \alpha e(n)\mathbf{x}(n) \tag{2}$$

The computational load is twice that due to implementation of the FIR filter.

The normalised LMS algorithm compensated for changes in the amplitude of the input signal, $x(n)$, to give a constant rate of convergence even when the input signal power fluctuates (equation (3)).

$$\mathbf{w}(n+1) = \mathbf{w}(n) + \frac{\alpha}{\mathbf{x}^T\mathbf{x}} e(n)\mathbf{x}(n) \tag{3}$$

Parametric adaptation algorithm

The NLMS algorithm is easy to implement, but may not be able to converge fast enough to track rapid changes in the feedback path, thus causing the hearing aid system to become unstable. The aim of this project is to develop a system of adaptive feedback cancellation which is robust to changes in the feedback path, i.e. will not become unstable when the feedback path changes. In order to minimise the likelihood of instability, the algorithm should be able to track rapid changes in the feedback path. This requires the algorithm to converge quickly. Better tracking of changes will allow better cancellation of the feedback path, and hence allow higher gains to be used before the onset of oscillation, increasing the usefulness of the hearing aid to patients with severe and profound hearing loss.

The algorithm developed here uses prior knowledge of the hearing aid system obtained from a computer model. This model allows investigation of the components of the system, finding which parameters are constant after fitting the device to the patient and which vary, leading to variations in the feedback path response. For simplification, the presence of slit leakage around the earmould was included in the model of the vent, rather than modelling the leak as a second tube in parallel with the vent.

In the examples given in this report, the combined vent/leak tube was the only varying part of the hearing aid system; all other parts were kept constant. Varying a single parameter is the simplest situation. First, we shall consider the varying vent/leak radius, simulating an increasing amount of sound leaking around the earmould from the receiver to the microphone.

Varying the combined vent/leak radius

Consider the vent and leak as two tubes of the same length and with the same distance from the tube exit to the microphone input. The radius of the vent, r_v, and leak, r_l, are combined. If the cross-sectional area of the combined tube is given by:

$$\pi r^2 = \pi r_v^2 + \pi r_l^2 \tag{4}$$

then

$$r^2 = r_v^2 + r_l^2 \tag{5}$$

and

$$r = \sqrt{r_v^2 + r_l^2} \tag{6}$$

A set of MATLAB programs and functions were written to calculate the response of the feedback path from the receiver input to the microphone output. The basis of the programs was the calculation of the 2 x 2 matrix describing the feedback path from two-port network equations for the tubes and transducers:

$$\begin{bmatrix} A_{total} & B_{total} \\ C_{total} & D_{total} \end{bmatrix} = \begin{bmatrix} A_r & B_r \\ C_r & D_r \end{bmatrix} \begin{bmatrix} A_1 & B_1 \\ C_1 & D_1 \end{bmatrix} \begin{bmatrix} A_2 & B_2 \\ C_2 & D_2 \end{bmatrix} \begin{bmatrix} 1 & 0 \\ 1/Z_T & 1 \end{bmatrix} \begin{bmatrix} A_3 & B_3 \\ C_3 & D_3 \end{bmatrix} \begin{bmatrix} 1 & 0 \\ 1/Z_V & 1 \end{bmatrix} \begin{bmatrix} A_F & B_F \\ C_F & D_F \end{bmatrix} \begin{bmatrix} A_m & B_m \\ C_m & D_m \end{bmatrix} \quad (7)$$

The subscript r denoted the two-port network parameters of the receiver, 1 the receiver tube, 2 the ear canal, T the tympanic membrane (eardrum), 3 the vent, V the vent exit, F the external acoustic feedback path and m the microphone. The response of the feedback path is given by $1/A_{total}$.

It was possible to derive a simplified expression for A_{total}:

$$A'_{total} = A_m\left(A_r Z_1 \sinh(\Gamma_1 L_1) + B_r \cosh(\Gamma_1 L_1)\right)\left\{\frac{Z_3 \sinh(\Gamma_3 L_3)}{\left(Z_T \cosh(\Gamma_2 L_2) + Z_2 \sinh(\Gamma_2 L_2)\right) \Big/ \left(\frac{Z_T \sinh(\Gamma_2 L_2)}{Z_2} + \cosh(\Gamma_2 L_2)\right)}\right\}\frac{2R\pi}{\rho_0 cke^{j\left(\frac{\pi}{2} - kR\right)}} \quad (8)$$

A block diagram of the parametric adaptation algorithm is shown in figure 3 below.

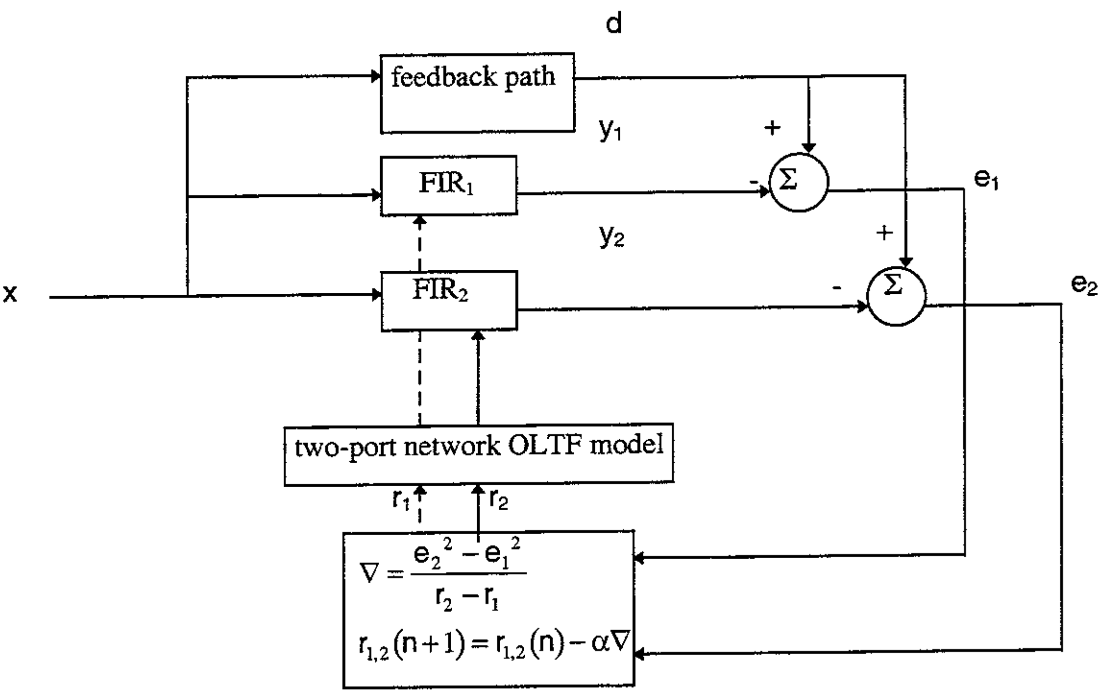

Figure 3: Block diagram of the parametric adaptation algorithm.

The frequency response of the open-loop transfer function from the microphone input to the output of the external path was calculated using matrix multiplication or equation (8) (recalculated for the microphone-to-external path matrix configuration, which results in a slightly different form for the expression), and used to derive the coefficients of a 512-point finite impulse response (FIR) filter using the inverse Fast Fourier Transform (FFT). This was done for the actual feedback path before and after a change in the radius of the combined vent/leak, r_{fb}, and hence in the feedback path. This simulated a change in the amount of acoustic leakage around the earmould from the receiver to the microphone. Two filters, FIR_1 and FIR_2, were derived from the feedback path responses produced with estimates of the radius given by $r_{fb1} \pm 0.25$ mm, where r_{fb1} was the radius of the combined vent/leak in the initial actual feedback path. In this example, r_{fb1} was 1.204 mm and r_{fb2} was 4.176 mm, representing a 1.2 mm radius vent and an effective leak radius changing from 0.1 mm to 4 mm.

The errors were given by:

$$e_1 = d - y_1 \tag{9}$$

$$e_2 = d - y_2 \tag{10}$$

e_1 and e_2 are the error signals due to the difference between the desired signal d and the estimated signals y_1 and y_2, respectively.

The error signals were used to calculate an approximated gradient of the instantaneous error and update r_1 and r_2:

$$\nabla = \frac{e_2^{\,2} - e_1^{\,2}}{r_2 - r_1} \tag{11}$$

$$r_{1,2}(n+1) = r_{1,2}(n) - \alpha\nabla \tag{12}$$

α is the convergence coefficient.

The new values of r_1 and r_2 were used to calculate new estimates of the feedback path response. After a number of iterations, the response calculated using the mean value r_{est} should be close to the actual feedback path response. r_{est} is given by:

$$r_{est} = \frac{r_1 + r_2}{2} \tag{13}$$

The feedback path response was modelled over the frequency range 1 Hz to 20 kHz and sampled at 40 kHz. The FIR filter coefficients were obtained by taking the inverse Fast Fourier Transform of the response. A 512-point filter was used. When plotting the responses of the FIR filters, the filter was zero padded to 1024 points and the FFT taken. The performance of the parametric adaptation algorithm was compared with that of the normalised LMS (NLMS) algorithm [Widrow and Stearns, 1985]. The program ran for 100 iterations.

After 100 iterations, i.e. 88 iterations after the feedback path changed, it can be seen that the responses of FIR_1 and FIR_2 lie either side of that of the final feedback path (see figure 4). For this simulation, the final values of r_1 and r_2 were 3.944 mm and 4.444 mm respectively. Figure 5 shows the response of the estimated feedback path, with r_{est} = 4.194 mm. The actual feedback path used r_{fb2} = 4.176 mm. Excellent agreement is seem between the estimated and actual final feedback paths. However, the NLMS algorithm has not converged to a reasonable estimate of the feedback path.

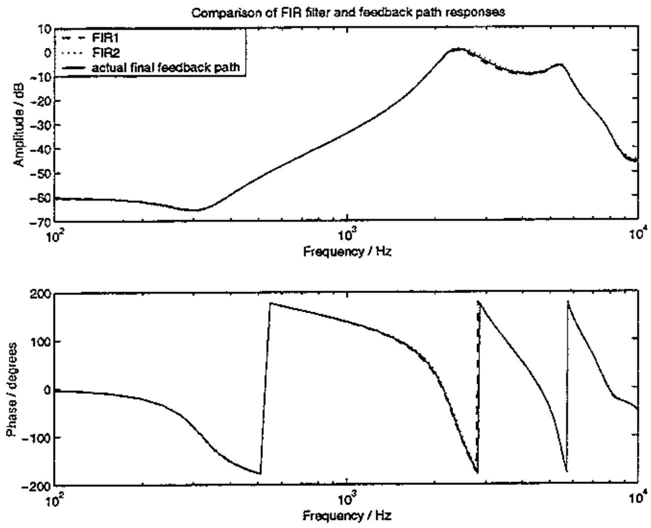

Figure 4: Comparison of FIR filter responses with actual final feedback path response.

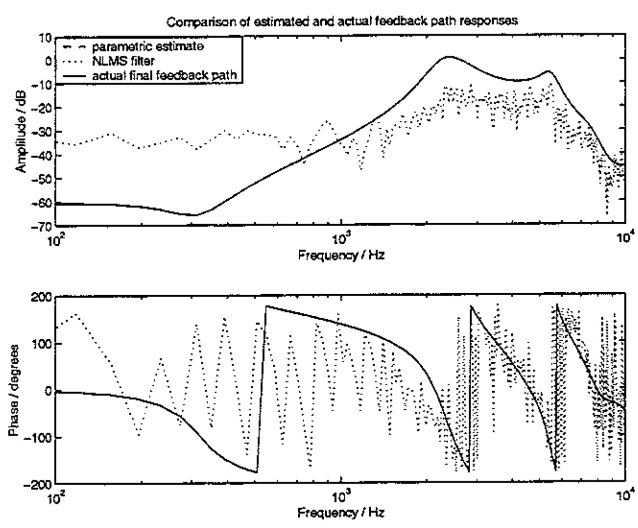

Figure 5: Comparison of estimated and actual feedback path responses with NLMS filter response.

Looking at the error signals for both the parametric algorithm and the NLMS, it can be seen that the errors are much smaller for the parametric algorithm than for the NLMS (figure 6).

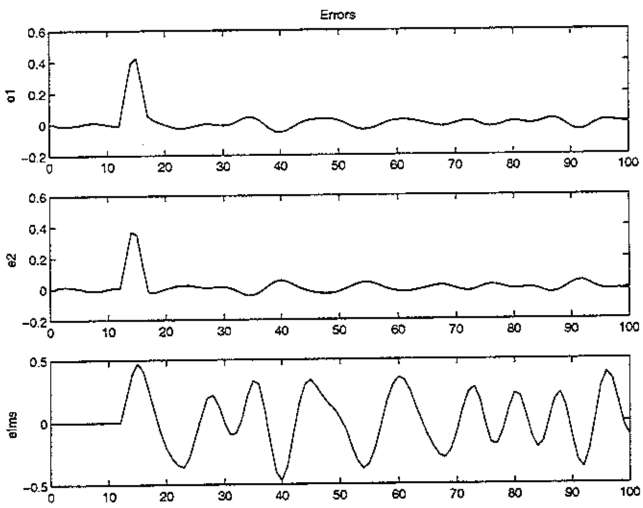

Figure 6: Error signals for parametric and NLMS algorithms.

The convergence behaviour of the parametric algorithm can be seen more clearly by plotting the estimated radius against the number of iterations (figure 7). It can be seen that the radius matches that of the actual feedback path before the feedback path is changed after the twelfth iteration. The estimated radius converges to the new feedback path radius after about 8 iterations after the feedback path changes.

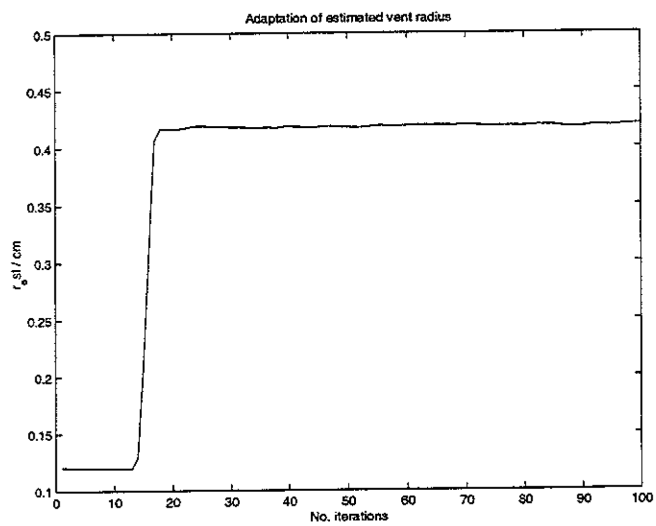

Figure 7: Convergence behaviour of the estimated vent / leak radius.

Compare this with the behaviour of the NLMS algorithm. After 8000 iterations, the NLMS response is in good agreement with the actual feedback path (figure 8). It can be seen from the error signal that the algorithm has only just converged (figure 9).

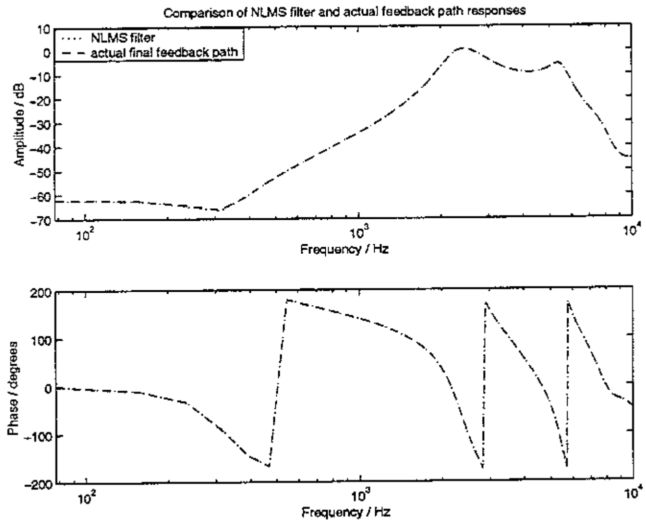

Figure 8: Comparison of actual feedback path and NLMS filter responses after 8000 iterations.

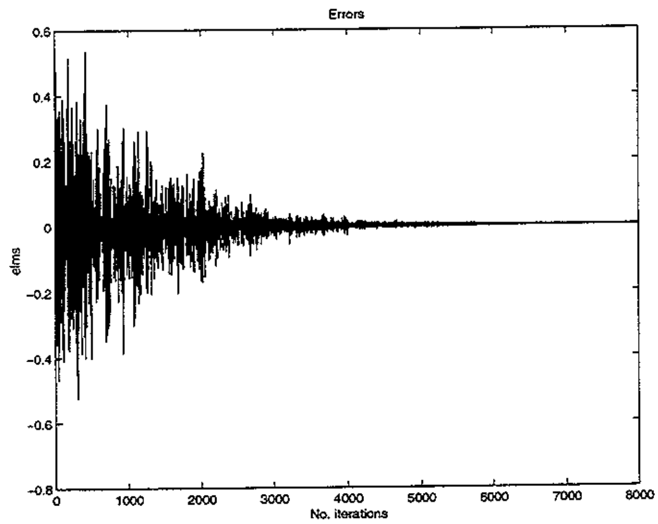

Figure 9: Convergence of NLMS error signal.

The mean error signal obtained with the parametric adaptation is compared with that of the NLMS for the first 100 iterations in figure 10. It can be seen that the parametric algorithm results in a smaller error as well as faster convergence.

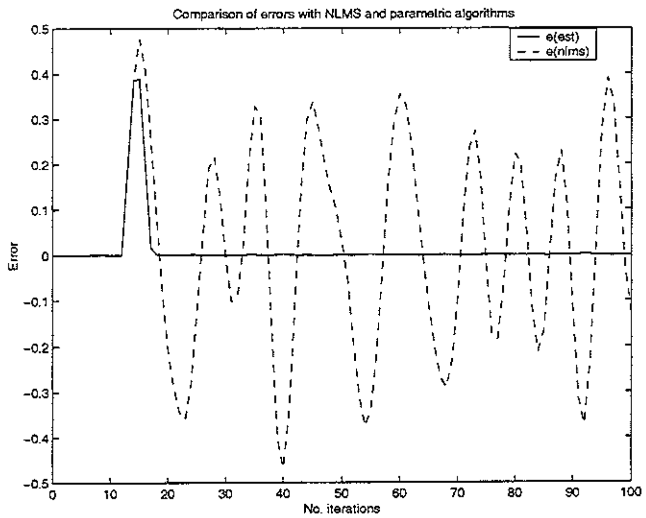

Figure 10: Comparison of parametric algorithm and NLMS error signals.

The error surface for the varying radius parametric adaptation algorithm is shown in figure 11. It can be seen that the surface is unimodal, i.e. it has a single minimum, so the algorithm will converge to a unique value. The steep sides of the error surface either side of the minimum indicate fast convergence, supporting the observations made above.

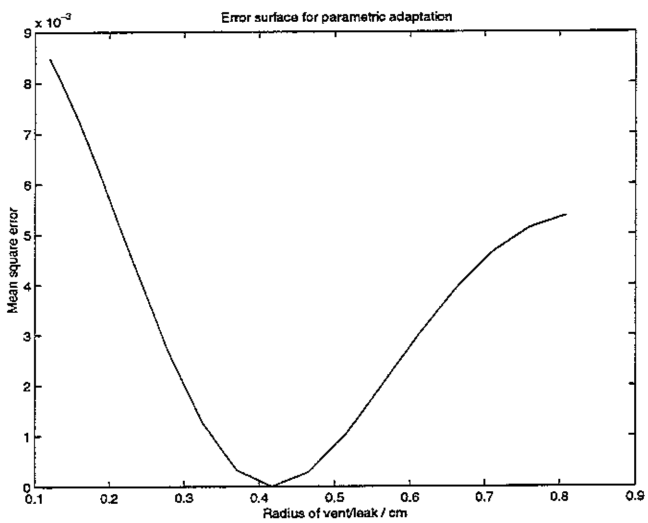

Figure 11: Error surface of the parametric adaptation algorithm.

If we examine the impulse response of the feedback path (see figure 12), it can be seen that a 256 point filter will be adequate.

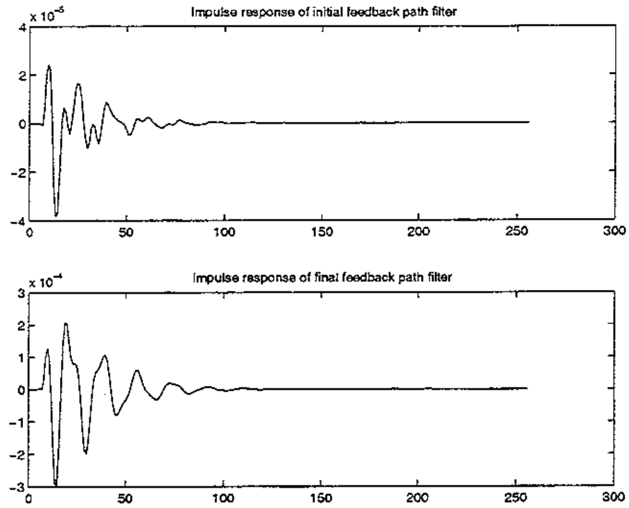

Figure 12: Impulse response of the feedback path.

Considering the NLMS algorithm alone, good agreement was achieved between the NLMS filter response and the actual feedback path response after 4000 iterations using a 256 point FIR filter (figure 13).

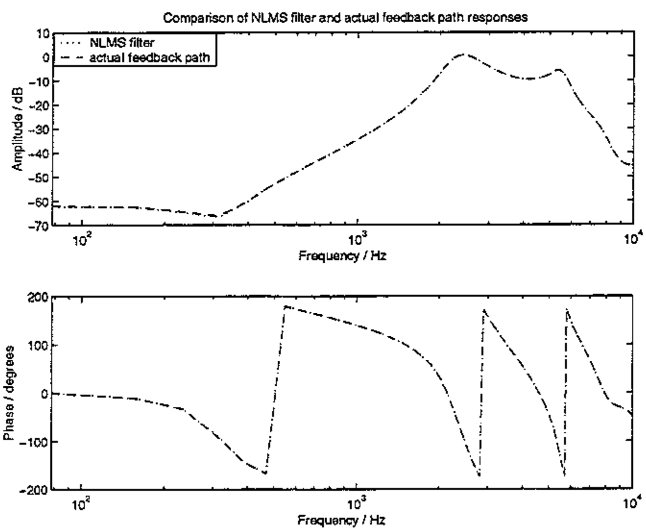

Figure 13: Comparison of the NLMS filter response after 4000 iterations with the actual feedback path response.

Examining the error signal, it can be seen that convergence has occurred after 4000 iterations (figure 14).

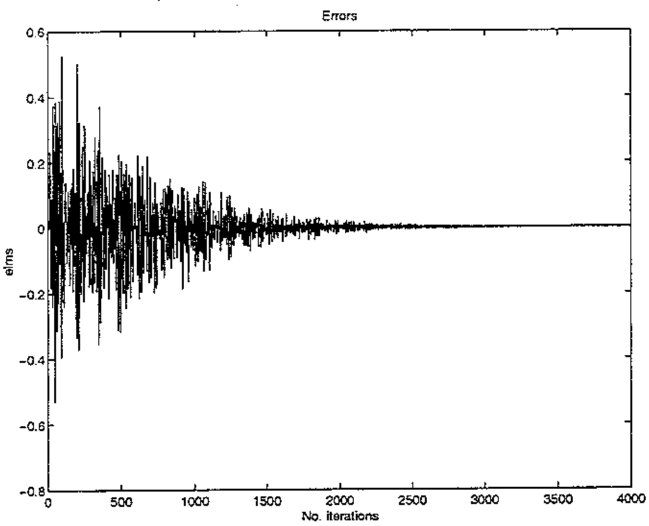

Figure 14: Convergence behaviour of the NLMS error signal.

The mean square of the NLMS filter coefficients appears to have converged after about 3000 iterations (figure 15).

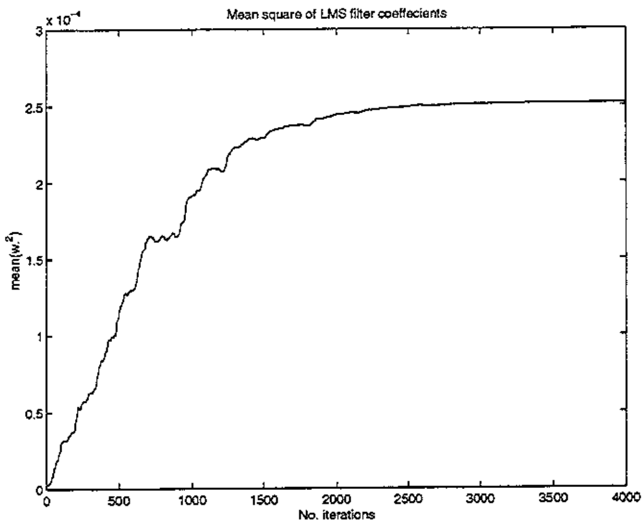

Figure 15: Convergence behaviour of the mean square of the NLMS filter coefficients.

Therefore the performance of the NLMS algorithm can be improved by using a shorter filter length.

Comparing the convergence behaviour of the estimated vent / leak radius for the parametric adaptation algorithm (calculated with 256 point filters, zero padded to 512 points when plotting the FFT for the frequency response curves) and the mean square NLMS filter coefficients (scaled up to appear on the same axes) (figure 16), it can be seen that the parametric algorithm converges after about 8 iterations while the NLMS algorithm takes about 3000 iterations. Therefore the parametric adaptation algorithm is two orders of magnitude faster than the NLMS algorithm for this particular application, even using shorter filter lengths.

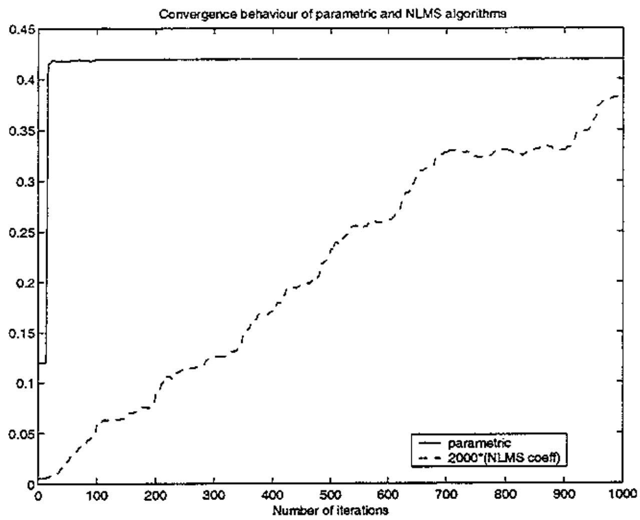

Figure 16: Comparison of the convergence behaviour of the parametric adaptation and NLMS algorithms.

Varying the combined vent/leak length

A second example varied the length of the combined vent and leak, keeping all other parameters constant, including the vent/leak radius. The algorithm had the same form as before, replacing the radius r with the length L. However, a different convergence coefficient was required. In the example shown below, $\alpha = 10$. The modelled feedback path was the measurable path from the receiver input to the microphone output with 50 dB arbitrary gain, representing the hearing aid amplifier, and was calculated with the analytic expression given by equation (8) rather than by matrix multiplication. This illustrates that both methods are valid, though the analytic expression is preferable as it reduces the computational load of the algorithm.

The initial feedback path was calculated with a combined vent/leak length, L_{fb1}, of 1.2 cm. After 12 iterations, the feedback path was changed to that calculated with $L_{fb2} = 1.7$ cm. As before, the response of the NLMS filter before adaptation was the same as that of the initial feedback path. Initially, FIR_1 and FIR_2 were obtained for $L_1 = L_{fb1} - 0.05$ cm and $L_2 = L_{fb1} + 0.05$ cm, respectively.

After 100 iterations (88 iterations after the feedback path changed), it was found that the responses of FIR_1 and FIR_2 lay close to that of the actual feedback path (figure 17). The main difference showed in the frequency of the peak near 9 kHz, which is governed by the vent/leak length. For this simulation, the final values of L_1 and L_2 were 1.65 cm and 1.75 cm respectively, giving a mean estimated length, L_{est}, of 1.7 cm, which is in exact agreement with the actual length, L_{fb2}. Thus, exact agreement was observed between the estimated and actual final feedback paths (figure 18 - note that the parametric estimate and actual feedback path responses appear as a single response due to the exact agreement). However, it can be seen that the NLMS algorithm has not converged to a reasonable estimate of the feedback path response 88 iterations after the path changed.

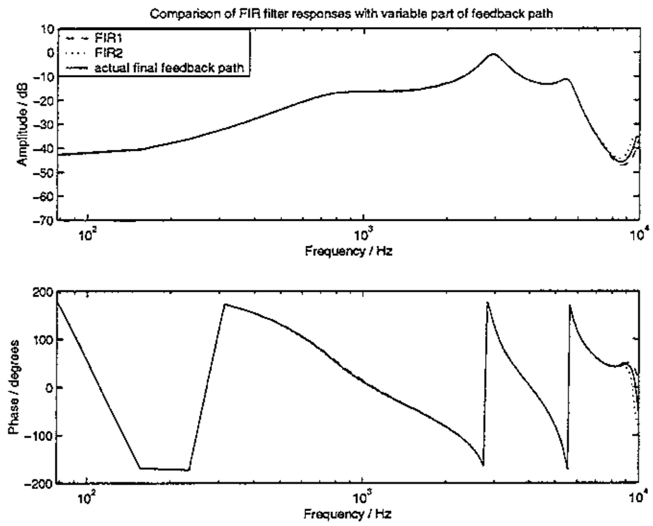

Figure 17: Comparison of FIR filter responses with response of actual final feedback path.

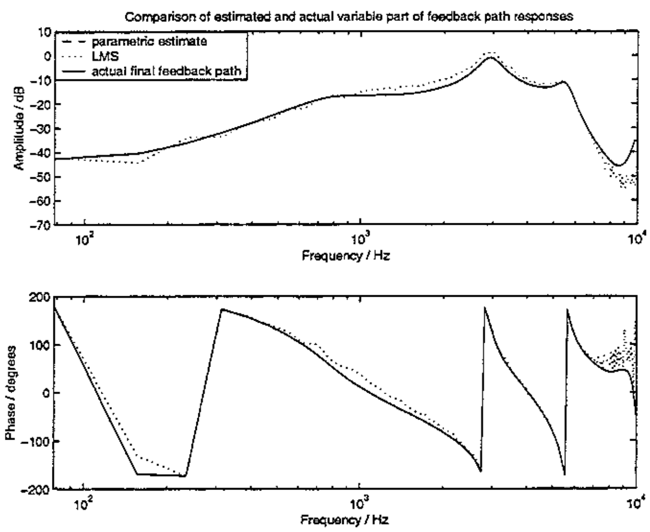

Figure 18: Comparison of parametrically-estimated and actual feedback path responses with NLMS filter response 88 iterations after the change in the feedback path.

Considering the error signals for both the parametric algorithm and the NLMS, it was found that the errors were about ten times smaller for the parametric algorithm. This can be seen clearly in figure 19, which compares the error signal produced by the parametric estimate, e_{est}, with the error produced by the NLMS algorithm, e_{nlms}. The parametric error has converged about fifteen iterations after the feedback path changed on the twelfth iteration. The NLMS algorithm had not converged after 100 iterations.

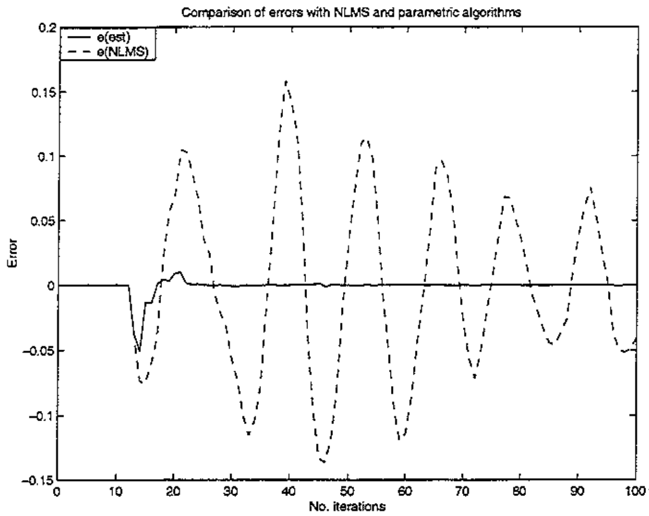

Figure 19: Comparison of error signals for parametric and NLMS algorithms

The convergence behaviour of the length-varying parametric algorithm is demonstrated by figure 20, which plots the estimated vent/leak length against the number of iterations. Initially, the estimated length fluctuates around the actual length before the feedback path changes on the twelfth iteration. These fluctuations are due to the random nature of the input signal and hence the error signals and gradient used to update the estimated length. The estimated length converges to the new value about 20 iterations after the feedback path changes.

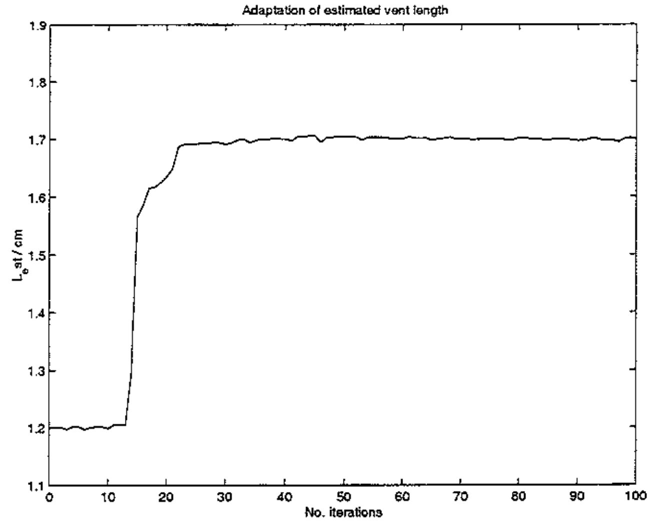

Figure 20: Convergence behaviour of the estimated vent/leak length.

The error surface for the varying length parametric adaptation algorithm is shown in figure 21. Again, the surface is unimodal, i.e. it has a single minimum, so the algorithm will converge to a unique value.

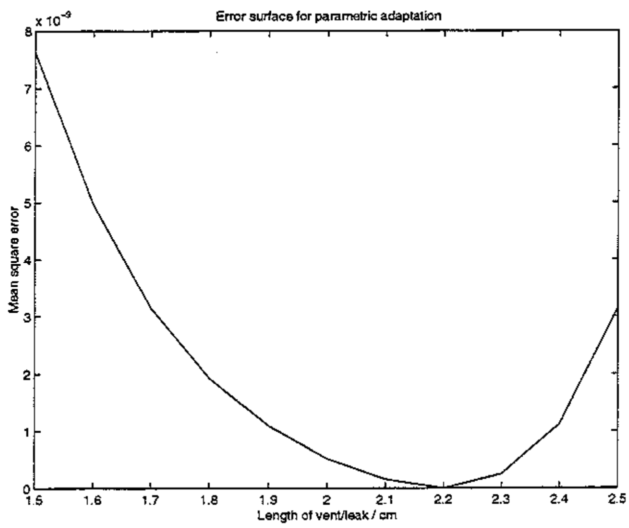

Figure 21: Error surface for the varying length parametric adaptation algorithm.

If we consider the NLMS algorithm, we find that good agreement was achieved between the NLMS filter and the actual feedback path responses after 4000 iterations using a 256-point FIR filter (figure 22). The error signal shows that convergence occurred after about 3000 iterations (figure 23), as does the plot of the mean square of the NLMS filter coefficients (figure 24). The performance is very similar to that observed when the feedback path altered following a change in the vent/leak radius, demonstrating that the performance of the NLMS algorithm was independent of the components of the hearing aid system, as expected.

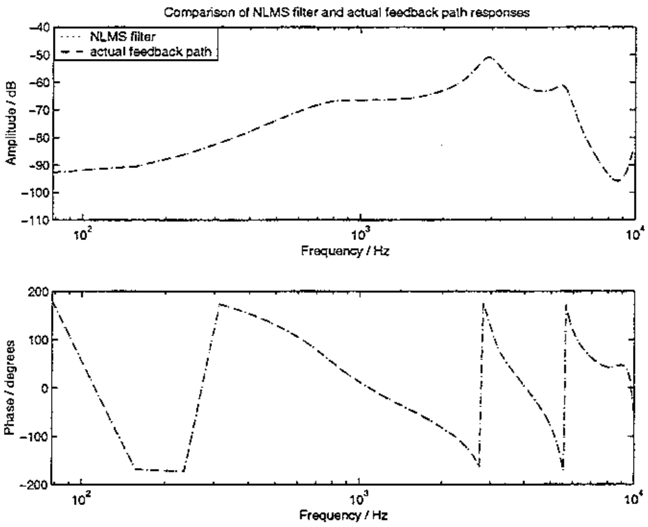

Figure 22: Comparison of NLMS filter response with actual feedback path response after 4000 iterations

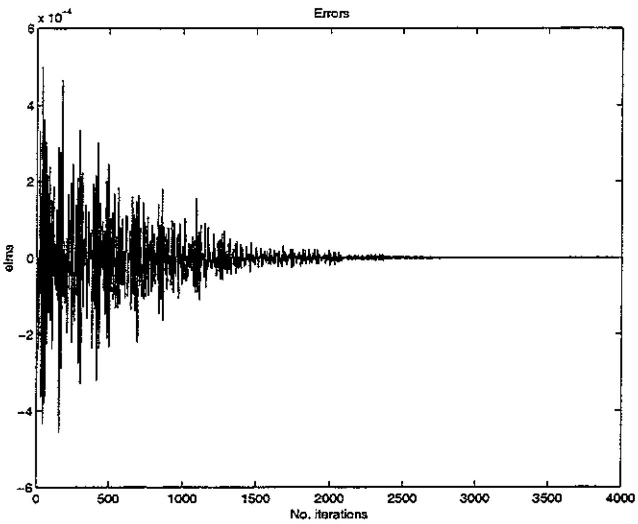

Figure 23: Convergence behaviour of the NLMS error signal

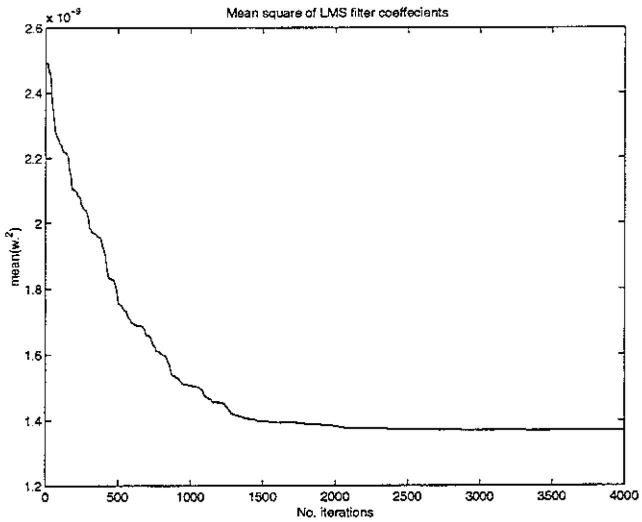

Figure 24: Convergence behaviour of the mean square of the NLMS filter coefficients

Computational efficiency

Although it has been demonstrated that the parametric algorithm converges in far fewer iterations than the normalised least mean squares algorithm with a white noise input signal, the actual running time is much greater. In order to use the parametric algorithm in a practical real time feedback cancellation system, the computational efficiency of the algorithm must be improved.

One strategy has been to derive a simplified expression for the feedback path response rather than calculating the response through matrix multiplication, thus reducing the computational load. Currently, refinements are being made to improve the performance of the algorithm further.

Future work

Although the work presented here deals with changes in the feedback path due to the variation of a single parameter, in reality variation may occur in several parameters simultaneously. Therefore the parametric algorithm must be expanded to process changes in more than one parameter.

A practical real-time parametric adaptation system will be developed. In its earliest stages, it is likely that this will be in the form of a hearing aid linked to a PC with digital signal processing capabilities. Eventually, it is intended that the algorithm should be implemented within the hardware of the hearing aid itself.

Conclusions

Taking into account the stochastic nature of the parametric algorithm, which causes the number of iterations required for convergence to vary, it has been demonstrated that in this simple case, varying a single parameter, the algorithm described in this report converges in far fewer iterations than the normalised LMS. This indicates that this is a promising approach to the problem of robust methods of feedback path cancellation.

The algorithm has been demonstrated for varying vent/leak radius and length, and will be extended to deal with simultaneous changes in more than one parameter. The computational efficiency of the algorithm will be improved and possible strategies for real-time implementation will be examined in future work.

References

1. Egolf, D.P., Haley, B.T., Howell, H.C., Legowski, S., Larson, V.D., "Simulating the open-loop transfer function as a means of understanding acoustic feedback in hearing aids", J. Acoust. Soc. Am., Vol. 85, No. 1, January 1989, pp. 454 - 467.
2. LoPresti, J.L., Carlson, E.V., "Electrical Analogs For Knowles Electronics, Inc. Transducers", Report No. 10531-3, Release 6, Knowles Electronics, Inc., 1151 Maplewood Drive, Itasca, IL 60143, 1999.
3. Widrow, B., Stearns, S.D., *Adaptive Signal Processing*, Englewood Cliffs, NJ: Prentice-Hall, 1985.